Original Article

A HYBRID EXPLAINABLE ARTIFICIAL INTELLIGENCE FRAMEWORK FOR ACCURATE TOTAL ORGANIC CARBON PREDICTION

Iorliam Aamo and Tyemimongo Iorlumun Cyprian
Department of Mathematics/Computer Science,
Rev. Fr. Moses Orshio Adasu University, Makurdi
(formerly, Benue State University, Makurdi), Nigeria.

ABSTRACT

Accurate estimation of Total Organic Carbon (TOC) is essential for evaluating source rock quality, hydrocarbon generation potential, and reservoir characterization. However, conventional TOC determination methods are often costly, time-consuming, and limited by data availability. This paper proposes an explainable hybrid machine learning and deep learning framework for reliable TOC prediction using petrophysical, elastic, and geochemical attributes derived from the Kolmani River-2 (KR-2) and Kolmani River-3 (KR-3) wells. Correlation analysis revealed strong nonlinear relationships among reservoir variables, highlighting the suitability of advanced data-driven modelling approaches. Four predictive models, namely Random Forest (RF), XGBoost, Decision Tree (DT), and Bidirectional Long Short-Term Memory (BiLSTM), were developed and evaluated. The results demonstrate that RF consistently outperformed the other models, achieving R^2 values of 0.9907 and 0.9977 for KR-2 and KR-3, respectively, with the lowest MAE, MSE, RMSE, and MAPE values. Ensemble learning methods showed superior predictive capability compared with deep learning, particularly for structured well-log datasets with limited sample sizes. To enhance model transparency, SHAP-based explainability analysis was employed, revealing Measured Depth (MD) as the most influential predictor, alongside ΔLogR, Gamma Ray, Neutron Porosity, TOC (Rk-Eval), and P-sonic. The proposed framework successfully combines predictive accuracy with interpretability, providing a robust and transparent solution.

KEYWORDS: **Total Organic Carbon (TOC); Explainable Artificial Intelligence (XAI); Machine Learning; Reservoir Characterization; Well-Log Analysis; Petrophysical Data Analytics.**

Open Access
Correspondence;
Iorliam Aamo

Email:
miorliam@yahoo.com

Citation: Iorliam Aamo and Tyemimongo Iorlumun Cyprian, *Department of Mathematics/Computer Science, Rev. Fr. Moses Orshio Adasu University, Makurdi (formerly, Benue State University, Makurdi), Nigeria*

Date of Publication:
Vol. 9 (1), 2026

pp 178-198

INTRODUCTION

The growing demand for accurate and interpretable total organic carbon (TOC) prediction has stimulated increasing interest in the integration of artificial intelligence (AI), machine learning (ML), and deep learning (DL) techniques, owing to their capability to model complex nonlinear relationships among petrophysical variables and support intelligent reservoir characterization. Longman *et al.* (2024) investigated the applicability of machine learning techniques for TOC prediction using well-log data from the Kolmani River-2 and Kolmani River-3 wells in Nigeria. Their study employed feature selection and nested cross-validation strategies and demonstrated that Random Forest and Naïve Bayes models can effectively estimate TOC, achieving coefficient of determination (R^2) values of 0.62 and 0.76. Aliouane and Ouadfeul (2025) examined the capability of Multilayer Perceptron (MLP) neural networks for predicting TOC and elemental capture spectroscopy (ECS) data from the Barnett Shale and Bakken oil fields. The results confirmed that neural network models can accurately reconstruct missing geochemical measurements and enhance reservoir characterization.

Recently, increasing attention has been directed toward explainable artificial intelligence (AI) for improving the transparency and reliability of predictive models. Miao *et al.* (2025) developed an explainable machine learning framework that combined advanced learning algorithms with interpretable AI techniques to provide reliable predictions and insights into feature contributions. Similarly, Zhang *et al.* (2026) proposed an interpretable framework for evaluating hydrogen adsorption capacity in shale reservoirs using machine learning models integrated with SHapley Additive exPlanations (SHAP). Their findings demonstrated that explainable models can achieve high predictive accuracy while simultaneously revealing the geological factors controlling reservoir behaviour. Jiang *et al.* (2026) further showed that machine learning-based frameworks can effectively predict production performance in offshore low-permeability reservoirs by incorporating reservoir heterogeneity into the modelling process.

Although previous studies have demonstrated the effectiveness of machine learning and deep learning approaches for TOC prediction and other reservoir-related applications, most existing frameworks rely on either standalone machine learning models or single deep learning architectures. Consequently, many of these models operate as black boxes, offering limited understanding of the influence of petrophysical variables on prediction outcomes. Furthermore, the integration of explainable artificial intelligence techniques into TOC prediction remains relatively unexplored. Therefore, there is a need for a robust framework capable of combining the predictive strengths of machine learning and deep learning while providing transparent and interpretable explanations of model decisions.

In this paper, an explainable hybrid machine learning and deep learning framework is proposed for accurate TOC prediction. The framework integrates feature engineering, Decision Tree, Random Forest, Extreme Gradient Boosting, and Bidirectional Long Short-Term Memory (BiLSTM) models with explainable artificial intelligence techniques, including SHapley

Additive exPlanations (SHAP) and Local Interpretable Model-Agnostic Explanations (LIME). The proposed approach aims to enhance prediction accuracy, improve model robustness, and transform TOC prediction from a black-box process into an interpretable decision-support system for reservoir characterization. The remainder of this paper is organized as follows: Section 2 presents the related literature, Section 3 describes the proposed methodology, Section 4 presents the results and discussions, and Section 5 presents the conclusion and future work.

REVIEW OF RELATED STUDIES

Longman *et al.* (2024) investigated the applicability of machine learning techniques for TOC prediction using well-log data from the Kolmani River-2 and Kolmani River-3 wells in Nigeria. The study employed exploratory data analysis, feature selection methods, and five-fold nested cross-validation to optimize regression and classification tasks. Several classification algorithms, including Logistic Regression, Decision Tree, K-Nearest Neighbour, Gradient Boosting, and Naïve Bayes, were evaluated, while Random Forest was used for regression. The prediction results yielded R^2 values of 0.62 and 0.76 with MSE values of 0.05 and 0.07, for the Kolmani River-2 and Kolmani River-3 wells datasets. Naïve Bayes achieved superior classification performance, demonstrating the effectiveness of machine learning for non-geochemical TOC prediction.

Aliouane and Ouadfeul (2025) investigated the effectiveness of Multilayer Perceptron (MLP) neural networks for predicting TOC and ECS data in unconventional reservoirs using well logs from the Barnett Shale and Bakken oil fields. The study employed standard logging parameters, including sonic, gamma-ray, resistivity, and neutron porosity logs, and evaluated several training algorithms, namely Hidden Weight Optimization, Conjugate Gradient, and Levenberg-Marquardt. Results demonstrated that MLP models can accurately estimate missing geochemical measurements and enhance reservoir characterization.

Miao *et al.* (2025) presented an explainable machine learning framework for predicting complex process variables using advanced data-driven techniques and interpretable artificial intelligence methods. Multiple machine learning algorithms were evaluated to capture nonlinear relationships among process parameters and improve predictive reliability. Feature engineering and model optimization were employed to enhance generalization performance, while explainability techniques provided insights into the contribution of individual variables. The proposed approach demonstrated superior prediction accuracy and robustness compared with conventional methods, highlighting the importance of interpretable models in industrial applications. The findings emphasized the potential of explainable machine learning for supporting efficient process optimization and reliable decision-making.

Zhang *et al.* (2026) developed an interpretable machine learning framework for evaluating hydrogen adsorption capacity in shale reservoirs to support underground hydrogen storage applications. Using 291 datasets comprising eight geological parameters, the authors compared Decision Tree, Random Forest, Gradient Boosting Decision Tree, and Artificial Neural

Network models integrated with SHapley Additive exPlanation (SHAP). The Random Forest model exhibited superior predictive performance, achieving R^2 values of 0.9948 and 0.9448 for the training and testing sets, respectively. SHAP analysis revealed that pressure, specific surface area, clay mineral content, and pore volume predominantly control hydrogen adsorption, providing valuable insights for optimizing shale reservoir selection and storage strategies.

Jiang *et al* (2026) proposed a machine learning-based framework for predicting production performance in offshore deep low-permeability and tight reservoirs through reservoir classification. Using production and reservoir data from the western South China Sea, the study integrated reservoir categorization with data-driven predictive models to capture the complex nonlinear relationships governing hydrocarbon production. By incorporating reservoir heterogeneity into the modelling process, the framework enhanced forecasting reliability and supported optimized field development strategies. The findings demonstrated the potential of artificial intelligence techniques for intelligent production prediction in complex reservoirs. The related literature reviewed in this paper is summarised in Table 1.

Despite significant advances in machine learning and deep learning for Total Organic Carbon (TOC) prediction and related reservoir applications, existing studies predominantly rely on either standalone machine learning models or single deep learning architectures, with limited emphasis on integrating both paradigms within a unified framework. Furthermore, most models remain black boxes, providing limited interpretability regarding the influence of geological and petrophysical variables on prediction outcomes. Although explainable artificial intelligence techniques have been explored in other domains, their application to TOC prediction remains scarce. Consequently, there is a need for a hybrid and explainable machine learning-deep learning framework capable of delivering improved prediction accuracy, robustness, and transparent decision-making for TOC estimation.

Table 1: Summary of Reviewed Literature

Author(s)	Findings	Techniques Adopted
Longman *et al.* (2024)	Machine learning techniques effectively predicted TOC from well-log data, with Random Forest achieving R^2 values of 0.62 and 0.76 and MSE values of 0.05 and 0.07 for the Kolmani River-2 and Kolmani River-3 datasets, respectively. Naïve Bayes provided the best classification performance.	Exploratory Data Analysis (EDA), feature selection, five-fold nested cross-validation, Logistic Regression, Decision Tree, K-Nearest Neighbour (KNN), Gradient Boosting, Naïve Bayes, and Random Forest.
Aliouane and Ouadfeul (2025)	MLP neural networks accurately estimated TOC and ECS values from well	MLP neural networks with Hidden Weight Optimization, Conjugate Gradient, and Levenberg-Marquardt

	logs, improving reservoir characterization and enabling prediction of missing geochemical measurements.	training algorithms.
Miao *et al*. (2025)	Explainable machine learning models enhanced prediction accuracy, robustness, and interpretability, demonstrating the importance of transparent decision-making in complex process modelling.	Explainable Artificial Intelligence (XAI), feature engineering, model optimization, and multiple machine learning algorithms.
Zhang *et al.* (2026)	Random Forest integrated with SHAP achieved excellent predictive performance (R^2 = 0.9948 and 0.9448 for training and testing datasets), while SHAP identified the key factors influencing hydrogen adsorption.	Decision Tree, Random Forest, Gradient Boosting Decision Tree (GBDT), Artificial Neural Network (ANN), and SHapley Additive exPlanation (SHAP).
Jiang *et al*. (2026)	Incorporating reservoir heterogeneity through reservoir classification improved prediction accuracy and reliability for production forecasting in deep low-permeability and tight reservoirs.	Reservoir classification and machine learning-based predictive modelling using production and reservoir data.

METHODOLOGY

This study proposes an explainable hybrid machine learning and deep learning framework for accurate Total Organic Carbon (TOC) prediction. The framework integrates feature engineering, ensemble learning, deep neural networks, and explainable artificial intelligence (XAI) techniques to improve prediction accuracy and enhance model interpretability. The overall methodology consists of data acquisition, preprocessing and feature engineering, hybrid model construction, explainability analysis, and model evaluation and optimal model selection.

A. Data Acquisition

Well-log and geochemical dataset from Longman *et al.* (2024) containing several petrophysical attributes and experimentally measured Total Organic Carbon (TOC) values are used in this experiment (i.e. TOC-ESTM (KR-2) and TOC-ESTM (KR-3)). The measured TOC served as the target variable, while the remaining variables constituted the predictor features. Preliminary statistical analysis and data inspection were performed to identify missing values, data inconsistencies, and irrelevant attributes.

B. Data Preprocessing and Feature Engineering

To improve data quality and ensure robust model development, Unnamed and irrelevant columns were removed from the dataset. Infinite values were replaced with missing values, while median imputation was employed to handle incomplete observations and preserve the statistical characteristics of the data. Thereafter, feature standardization was performed using the StandardScaler technique to eliminate scale variations among predictor variables. To further reduce dimensionality and improve model efficiency, Recursive Feature Elimination (RFE) based on Random Forest was employed to select the most informative features. The resulting feature subset was used for the model development.

C. Hybrid Model Construction and Implementation

Three machine learning algorithms were implemented which included Decision Tree (CART), Random Forest (RF), and Extreme Gradient Boosting (XGBoost). These algorithms were selected because of their ability to capture nonlinear relationships and their proven effectiveness in regression tasks.

For the deep learning model, a Bidirectional Long Short-Term Memory (BiLSTM) network was developed to model complex interactions among predictor variables. The architecture consisted of two bidirectional LSTM layers containing 64 and 32 neurons, respectively, followed by dropout regularization layers to mitigate overfitting. A dense hidden layer containing 16 neurons and a single output neuron were used to generate the final TOC prediction. The network parameters were optimized using the Adam optimizer, whereas Mean Squared Error (MSE) was adopted as the loss function. Early stopping was incorporated to prevent overtraining and improve generalization performance.

In order to move from black box to explainability, XAI techniques were integrated into the framework. Global model explanations were obtained using SHapley Additive exPlanations (SHAP), which quantified the contribution of each feature to the prediction process. SHAP summary plots, feature importance plots, and dependence plots were used to investigate the influence and interactions of predictor variables. Furthermore, local explanations were generated using SHAP waterfall plots and Local Interpretable Model-Agnostic Explanations (LIME), thereby enabling the interpretation of individual predictions. These explainability mechanisms transformed the prediction framework from a black-box model into a transparent and interpretable decision-support system.

D. Model Evaluation and Selection of the Optimal Predictor

The predictive performance of all models was evaluated using metrics such as the coefficient of determination (R^2), mean absolute error (MAE), mean squared error (MSE), root mean squared error (RMSE), and mean absolute percentage error (MAPE).

The graphical analyses used in this paper included actual vs predicted plots, prediction overlay curves, feature correlation heatmaps, and model comparison charts. The model exhibiting the highest coefficient of determination and the lowest prediction errors was selected as the optimal Total

Organic Carbon (TOC) prediction model. The entire methodology is summarised in Figure 1.

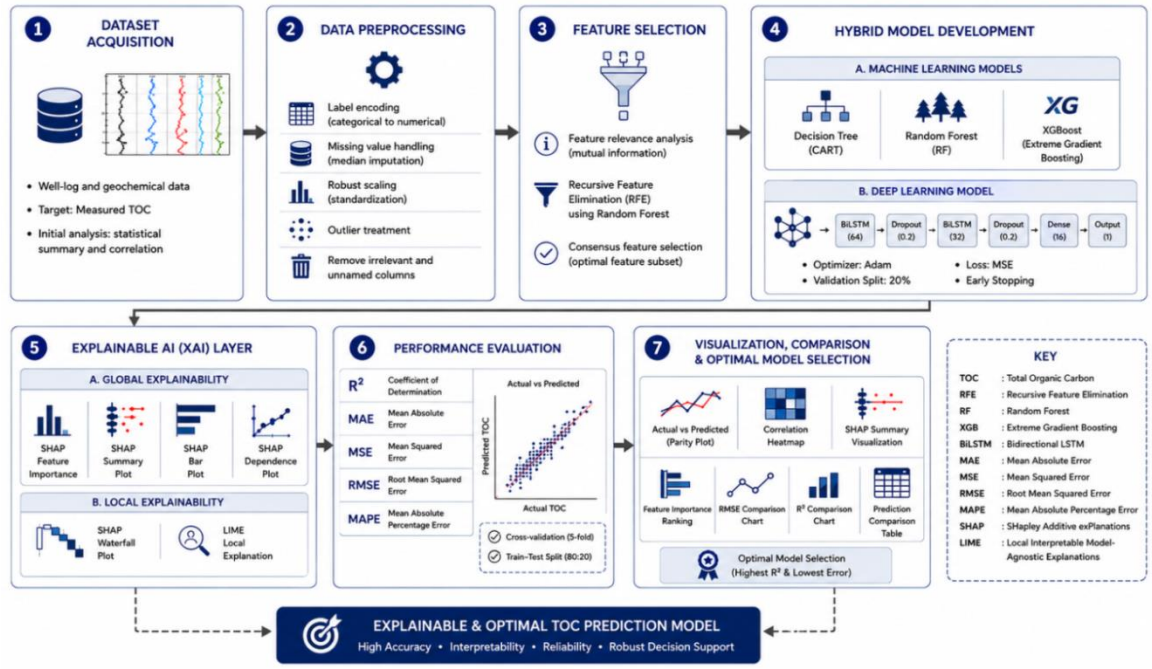


Figure 1: Schematic Diagram of the Proposed Methodology

RESULTS AND DISCUSSION

For the TOC-ESTM (KR-2), the feature correlation heatmap in Figure 2 reveals several important relationships among the petrophysical and TOC-related variables. Strong positive correlations are observed between gamma ray (GR), density transit time (DT), and neutron porosity (NEU), indicating that these logs capture similar geological characteristics associated with organic-rich formations. The transformed variables, particularly log10(RHOB), log10(DT), and log10(NEU), also exhibit moderate-to-strong positive correlations, suggesting that feature engineering successfully preserved meaningful reservoir information. Conversely, log10(Res) and the transformed porosity-related features display negative correlations, highlighting contrasting responses between resistivity and porosity indicators. Notably, the various TOC estimation methods exhibit very strong positive intercorrelations, confirming their consistency in representing organic matter content. The measured TOC shows strong associations with TOC estimates derived from GR, RHOB, NPHI, and DT logs, demonstrating the relevance of these petrophysical attributes for TOC prediction. In essence, the heatmap indicates the presence of significant nonlinear relationships and complementary feature interactions that can be effectively exploited by machine learning models to improve prediction accuracy and reservoir characterization.

Furthermore, the prediction models comparison is shown in Table 2 and Figures 4 and 5. For the predictive performance of the developed models for TOC-ESTM (KR-2) as shown in Table 2, the Random Forest (RF) model exhibited the best performance, achieving an R^2 value of 0.9907 and the

lowest prediction errors, with MAE, MSE, RMSE, and MAPE values of 0.0147, 0.0011, 0.0333, and 0.0180, respectively .

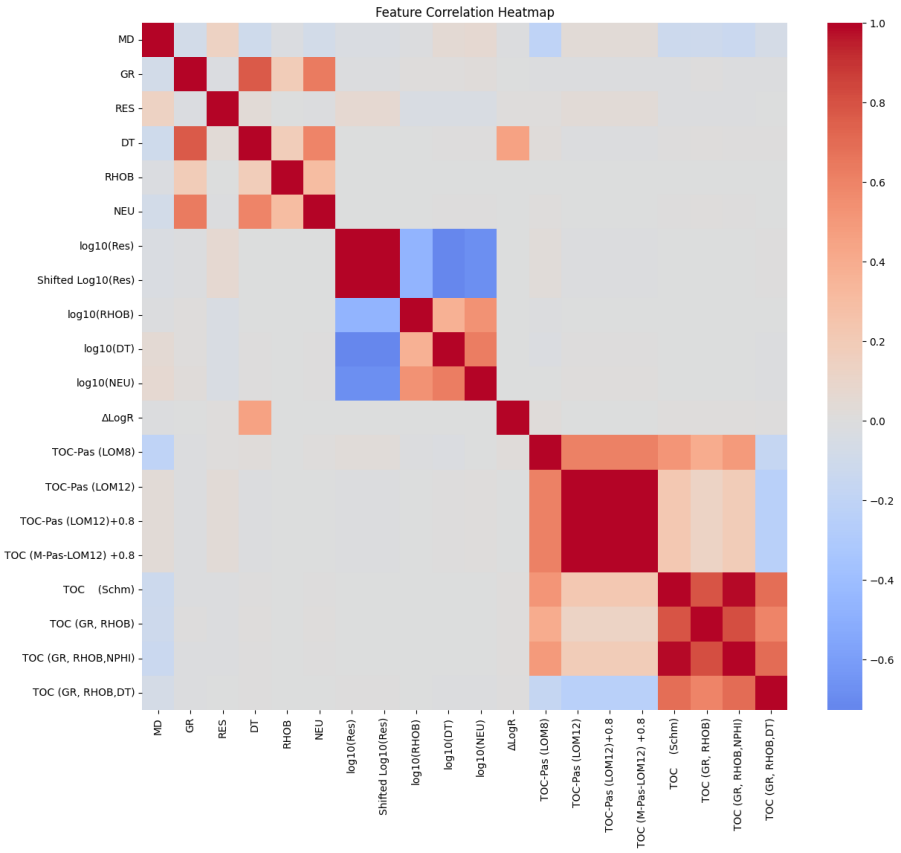


Figure 2: Feature Correlation Heatmap for TOC-ESTM (KR-2)

Table 2: Prediction Comparison of Models for TOC-ESTM (KR-2)

Model	**R2**	**MAE**	**MSE**	**RMSE**	**MAPE**
Random Forest	0.990702	0.014699	0.001110	0.033318	0.018037
Decision Tree	0.866724	0.076647	0.015912	0.126142	0.095216
XGBoost	0.830493	0.091688	0.020237	0.142258	0.113938
BiLSTM	0.504722	0.164004	0.059131	0.243169	0.197028

These results indicate that the ensemble learning mechanism of Random Forest effectively captured the complex nonlinear relationships among the petrophysical variables, resulting in highly accurate and robust TOC predictions.

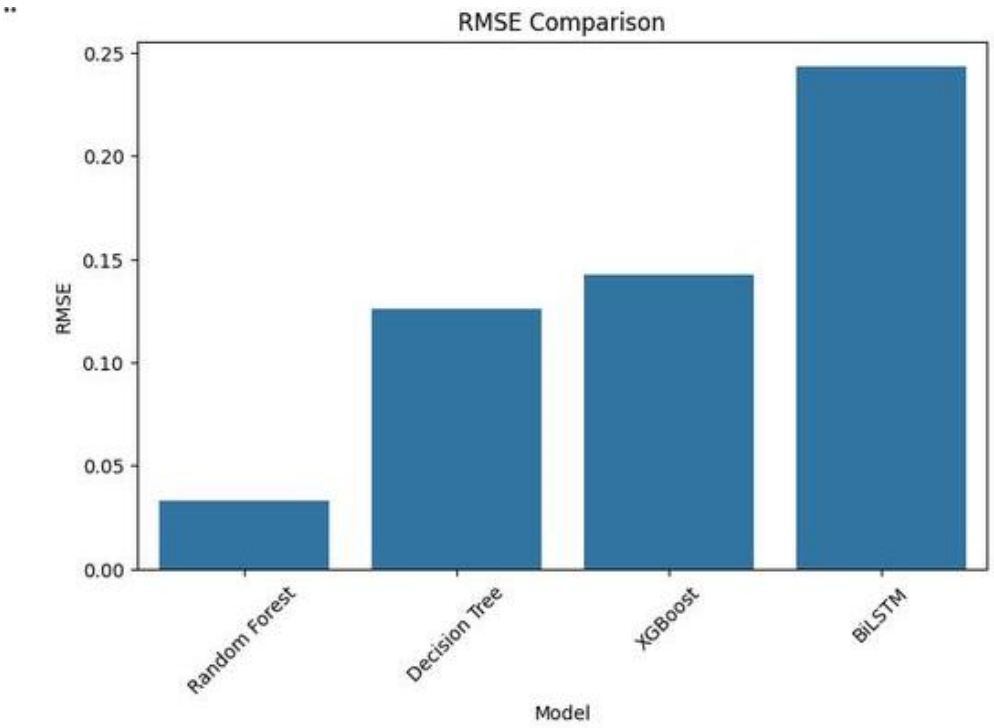
The Decision Tree model produced satisfactory results with an R^2 of 0.8667, although its prediction errors were considerably higher than those of Random Forest. This decline in performance can be attributed to the susceptibility of single-tree models to overfitting and their limited ability to generalize complex data patterns. Similarly, XGBoost achieved an R^2 value of 0.8305, accompanied by relatively larger error metrics, suggesting that despite its boosting strategy, the model was unable to

outperform the Random Forest algorithm for the considered dataset.

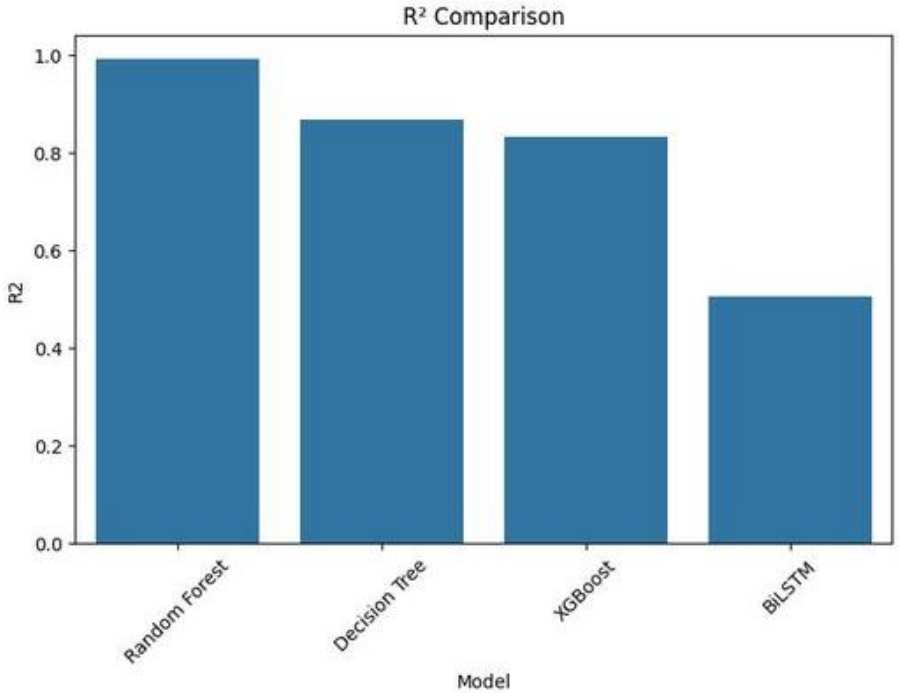
In contrast, the BiLSTM model yielded the weakest predictive performance, with an R^2 value of 0.5047 and the highest error measures. The poor performance of BiLSTM may be attributed to the limited size and non-sequential nature of the dataset, which restricted the network's ability to exploit temporal dependencies effectively. Overall, the TOC-ESTM (KR-2) results reveal that conventional ensemble learning approaches, particularly Random Forest, provide superior predictive capability for TOC estimation compared with both single-tree and deep learning models. The remarkably low prediction errors and excellent coefficient of determination further highlight the suitability of Random Forest as the optimal predictor for accurate and reliable TOC characterization.

To further show how the models predicted the values against the actual TOC values for TOC-ESTM (KR-2), Table 3 shows the comparison. For the fact that Random Forest came top, Figure 6 further shows the graphical comparison of the prediction.

To move from black-box predictions to explainability, we present the SHAP global feature importance as shown in Figure 7 and the SHAP waterfall plot as shown in Figure 8 for TOC-ESTM (KR-2).



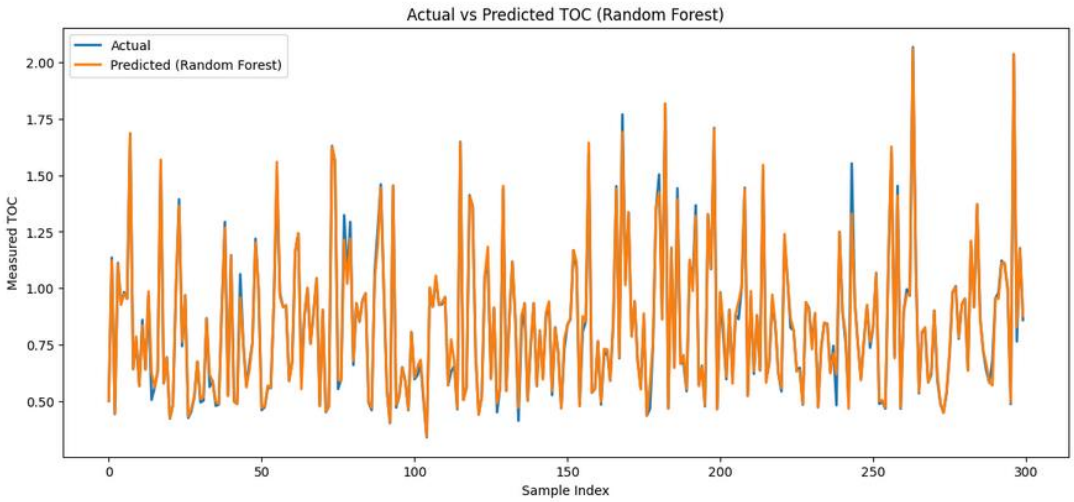
Figures 4: RMSE Comparison for Models for TOC-ESTM (KR-2)



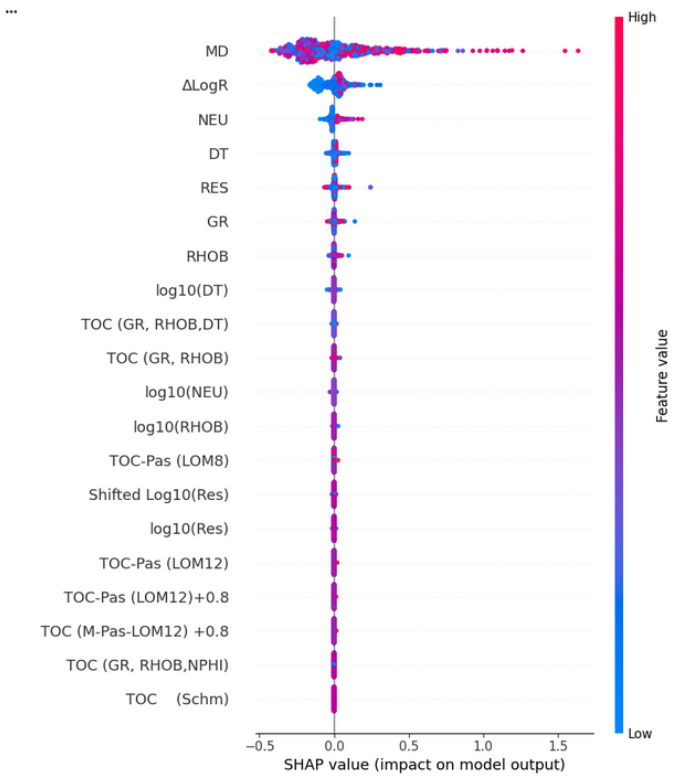
Figures 5: R2 Comparison for Models for TOC-ESTM (KR-2)

Table 3: Actual TOC VS Predicted TOC by Models for TOC-ESTM (KR-2)

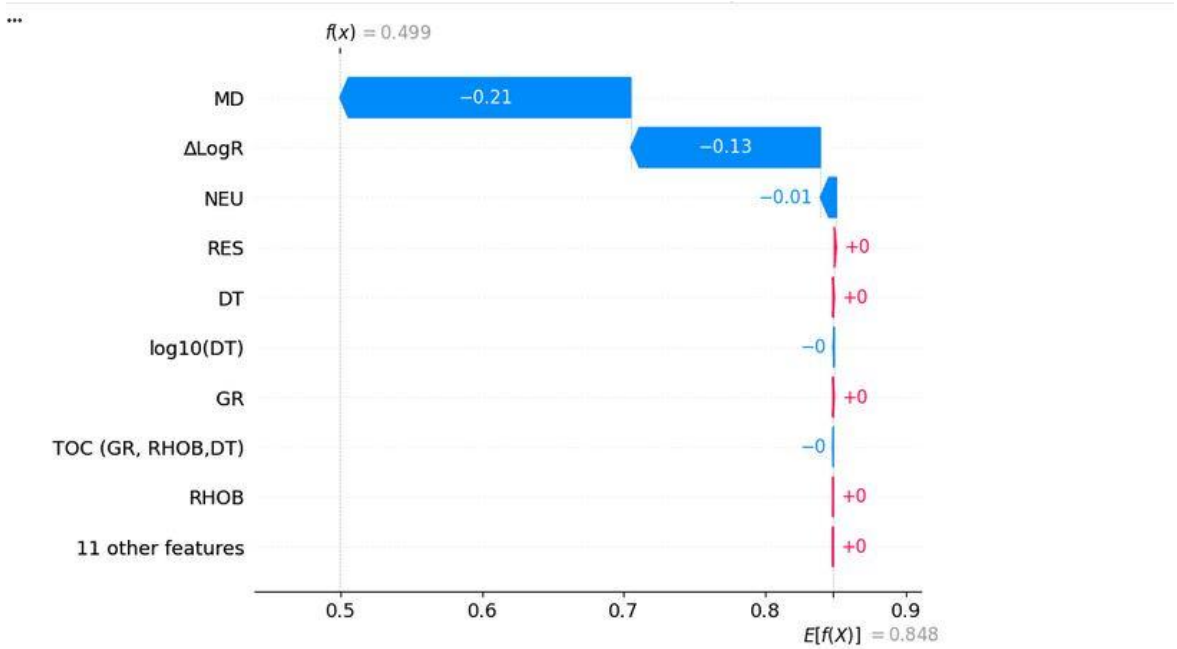
Actual TOC	Decision Tree	Random Forest	XGBoost	BiLSTM
0.499225	0.510628	0.499275	0.522856	0.619319
1.134950	1.130850	1.122222	1.071129	1.269715
0.441900	0.447695	0.444489	0.530522	0.519694
1.111550	1.132277	1.107727	1.099415	1.019276
0.927000	0.938449	0.927185	0.934171	0.958420



Figures 6: Actual VS Predicted Overlay by Random Forest for TOC-ESTM (KR-2)



Figures 7: SHAP Global Feature Importance for TOC-ESTM (KR-2)



Figures 8: SHAP Waterfall Plot for TOC-ESTM (KR-2)

The baseline prediction in Figure 8, represented by the expected value E[f(X)]=0.848, is progressively adjusted by the contributions of individual variables to produce the final prediction f(x)=0.499. The dominance of MD and ΔLogR indicates that these variables play a critical role in determining TOC predictions for this

observation. Furthermore, the plot demonstrates the effectiveness of SHAP in transforming the prediction process from a black-box mechanism into an interpretable framework, enabling transparent identification of the factors driving individual model decisions.

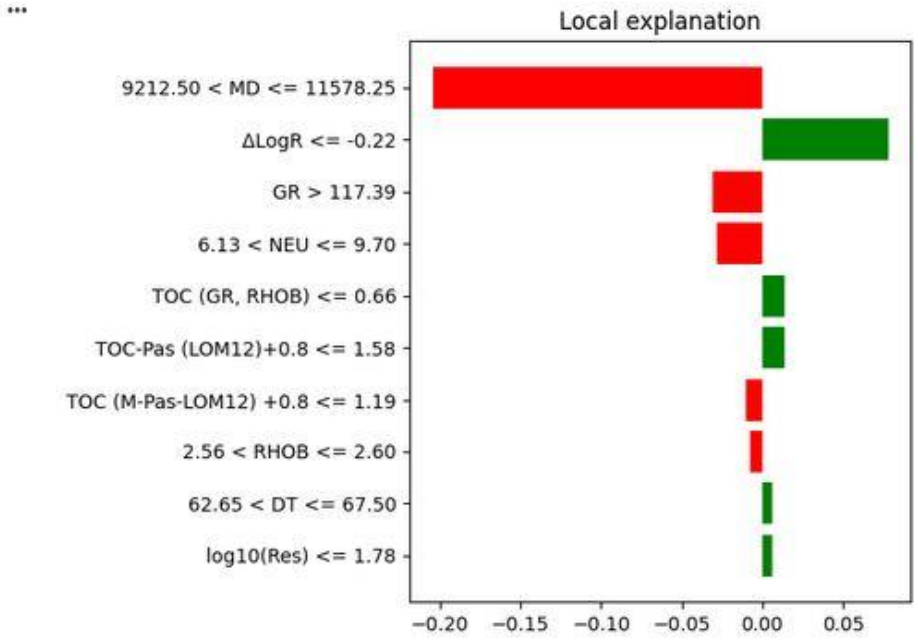
The local explanation plot for TOC-ESTM (KR-2) in Figure 9 provides instance-level interpretability by highlighting how individual features influence a specific TOC prediction. The results indicate that measured depth (MD) is the most influential variable, exerting a substantial negative contribution to the prediction when its value falls within the range of 9212.50–11578.25. In contrast, ΔLogR contributes positively and partially offsets the negative effect of MD, confirming its importance as an indicator of organic-rich intervals. Gamma ray (GR) and neutron porosity (NEU) also exhibit moderate negative influences, whereas variables such as TOC (GR, RHOB), TOC-Pas (LOM12)+0.8, transit time (DT), and log10(Res) contribute marginally to the final prediction. The mixture of positive and negative contributions demonstrates the complex interactions among geological and petrophysical parameters governing TOC estimation. Furthermore, the visualization confirms the effectiveness of local explainability techniques in identifying the specific drivers of individual predictions, thereby enhancing model transparency, trustworthiness, and practical applicability for reservoir characterization and decision support.

Overall, the explainability analysis identifies Measured Depth (MD), Delta Log Resistivity (ΔLogR), Gamma Ray (GR), and Neutron Porosity (NEU) as the primary controlling factors for accurate TOC estimation. This result agrees with Passey *et al.*, (2010), Szabó *et al.*, (2021), Valadez Vergara (2025), Allouti *et al.*, (2025), and Khan *et al.*, (2026).

The same experimental steps were carried out on TOC-ESTM (KR-3) and the rseults and discussion are presented as follows.

The feature correlation heatmap for the TOC-ESTM (KR-3) in Figure 10 shows strong positive correlations among RHOB, P-sonic, AI, S-impedance, P/S velocity ratio, Poisson's ratio, Lambda x Rho, and Mu x Rho, indicating that these elastic attributes capture similar rock-physics properties and reservoir characteristics. Log10(RES) exhibits a strong positive correlation with R90 and Mu x Rho but a negative relationship with neutron porosity, reflecting the contrasting responses of resistivity and pore-fluid effects. Notably, the TOC estimation variables show moderate-to-strong intercorrelations, confirming their consistency in representing organic matter content. The strongest TOC-related association is observed between TOC (M-Pas-LOM12) and TOC (M-Pas-LOM12)+0.8, indicating near-equivalent predictive behaviour. Furthermore, the negative correlation between the standard deviation metric and Passey-derived TOC estimates suggests reduced uncertainty in intervals with higher organic richness. Overall, the heatmap demonstrates the existence of complex multivariate relationships among reservoir attributes, highlighting the importance of advanced machine learning models capable of exploiting nonlinear feature interactions for accurate and reliable TOC prediction.

Again, the prediction models comparison for TOC-ESTM (KR-3) is shown in Table 3 and Figures 11 and 12.



Figures 9: LIME explanation for TOC-ESTM (KR-2)

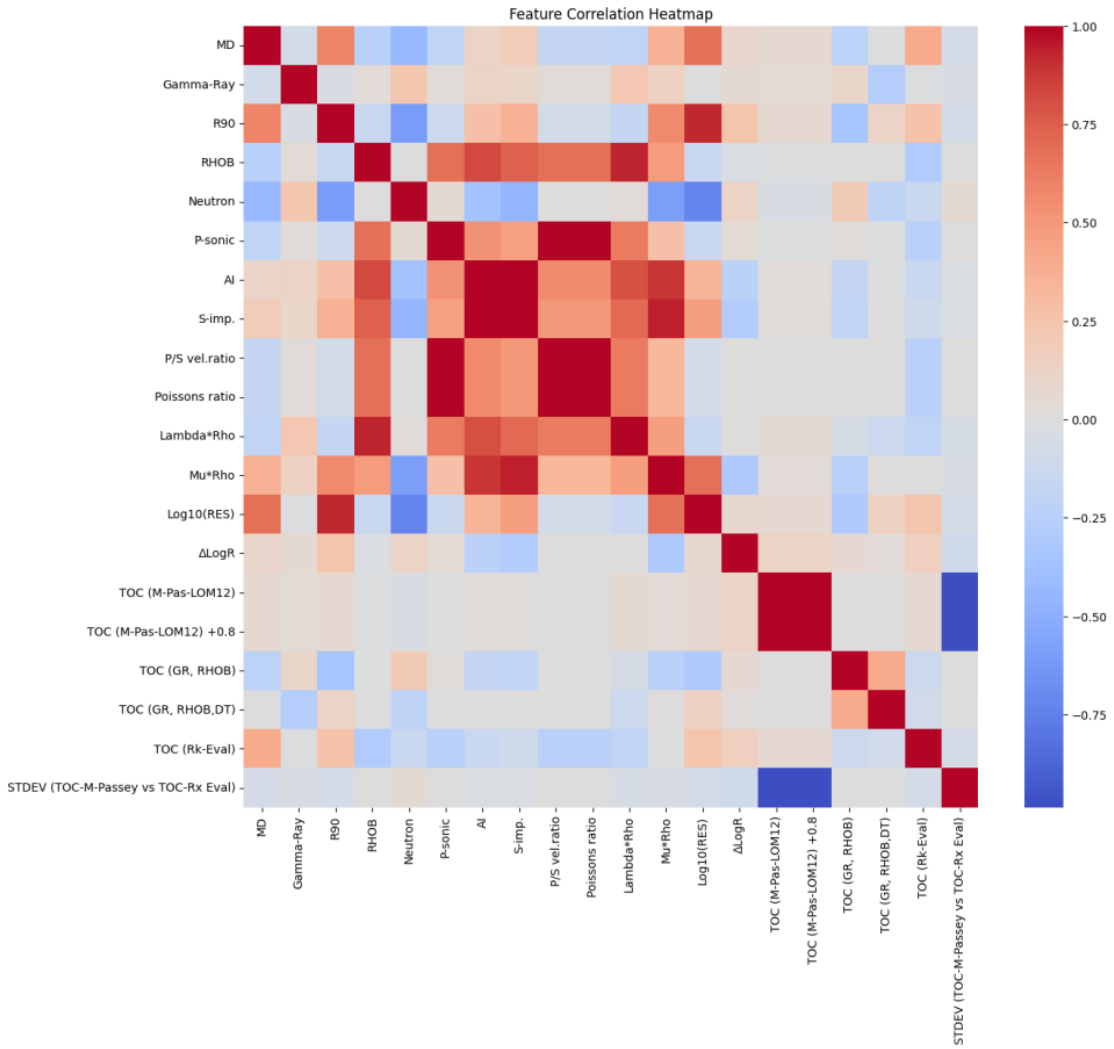


Figure 10: Feature Correlation Heatmap for TOC-ESTM (KR-3)

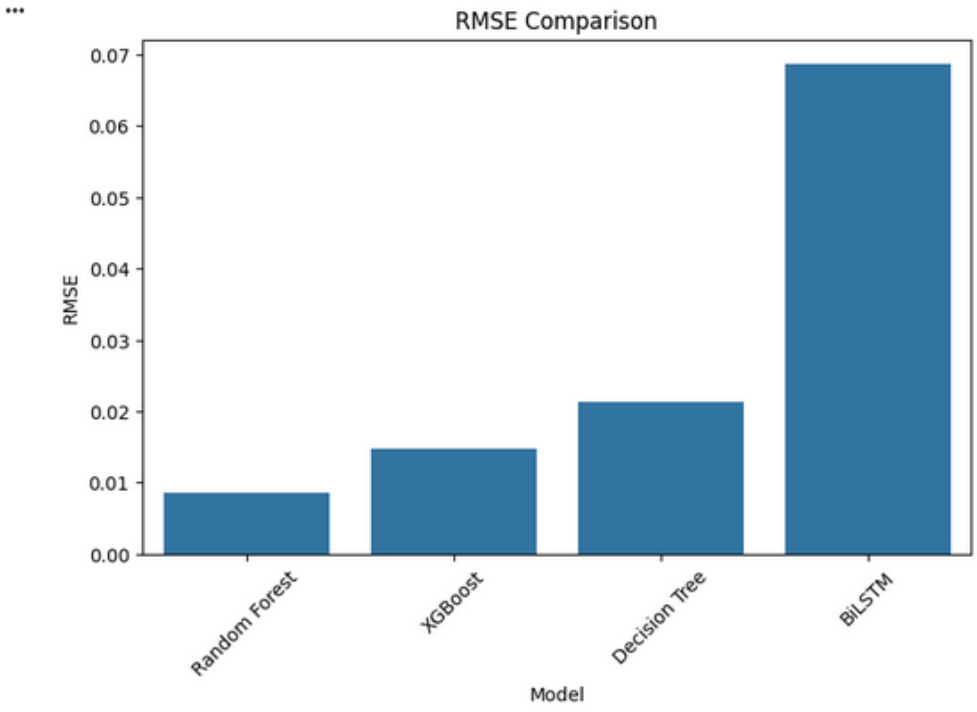
Table 3: Prediction Comparison of Models for TOC-ESTM (KR-3)

Model	R2	MAE	MSE	RMSE	MAPE
Random Forest	0.997692	0.002774	0.000075	0.008663	0.004066
XGBoost	0.993299	0.009870	0.000218	0.014760	0.016779
Decision Tree	0.986051	0.012164	0.000453	0.021295	0.020534
BiLSTM	0.855152	0.047034	0.004709	0.068622	0.082398

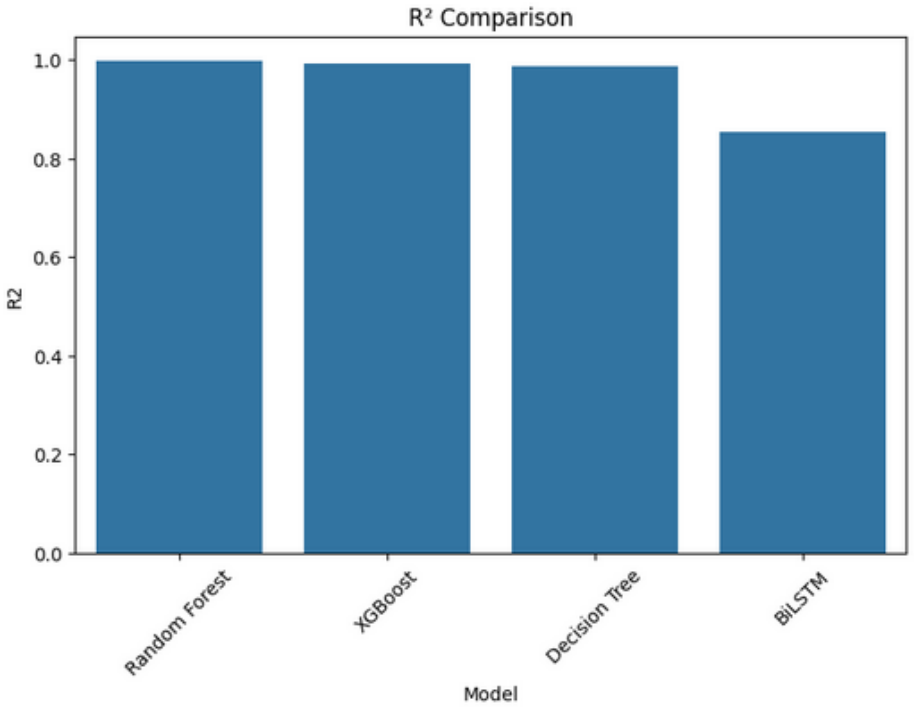
Table 3 demonstrate that Random Forest achieved the highest predictive accuracy (R^2 = 0.9977) and the lowest error metrics, indicating excellent capability in modelling complex TOC relationships. XGBoost and Decision Tree also performed strongly, whereas BiLSTM exhibited comparatively lower accuracy. Overall, ensemble learning methods significantly outperformed deep learning, highlighting their superior suitability for TOC prediction in the studied dataset.

The superior performance of Random Forest and XGBoost relative to BiLSTM can be attributed to the structured nature of the well-log dataset, the limited sample size, and the absence of pronounced sequential dependencies. Ensemble learning algorithms are particularly effective for tabular geoscience data because they capture complex nonlinear feature interactions while maintaining strong generalization capabilities. Conversely, BiLSTM networks typically require substantially larger datasets and sequential patterns to fully exploit their representational power (Zhang, Yan, Lai, and Wang, 2025).

To further show how the models predicted the values against the actual TOC values for TOC-ESTM (KR-3), Table 4 shows the comparison. For the fact that Random Forest came top, Figure 13 further shows the graphical comparison of the prediction.



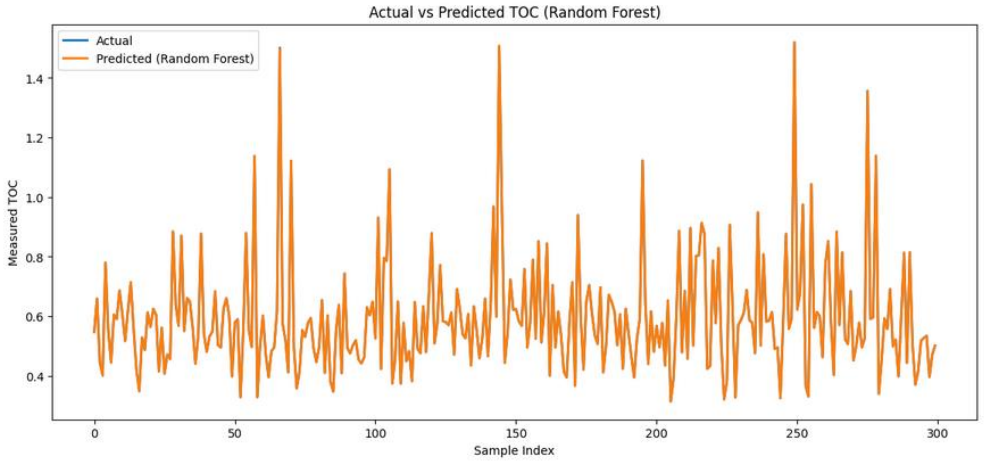
Figures 11: RMSE Comparison for Models for TOC-ESTM (KR-3)



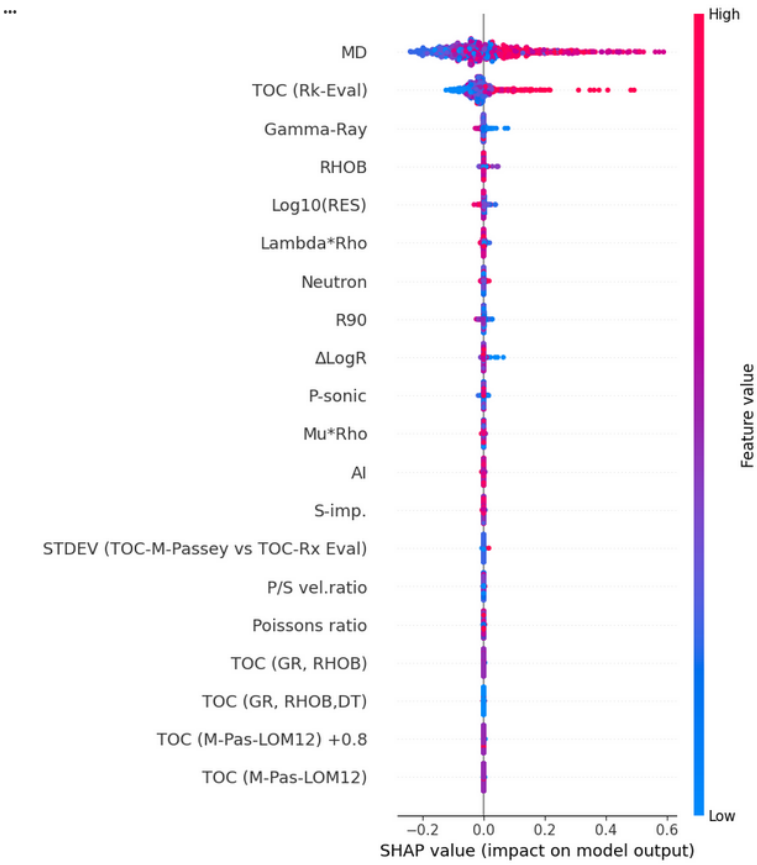
Figures 12: R^2 Comparison for Models for TOC-ESTM (KR-3)

Table 4: Actual TOC VS Predicted TOC by Models for TOC-ESTM (KR-3)

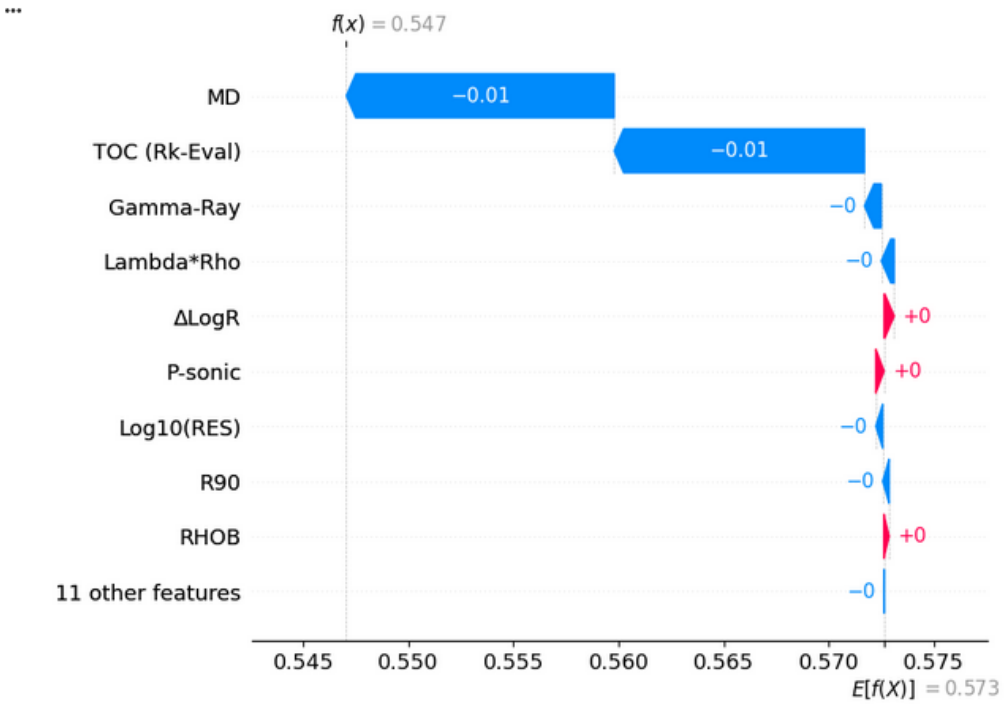
Actual TOC	Decision Tree	Random Forest	XGBoost	BiLSTM
0.546933	0.545761	0.547046	0.545637	0.541769
0.659500	0.661717	0.659361	0.662127	0.641945
0.444250	0.448975	0.443968	0.467710	0.478567
0.401333	0.400458	0.401390	0.409274	0.417605
0.780108	0.781394	0.788191	0.774883	0.765288



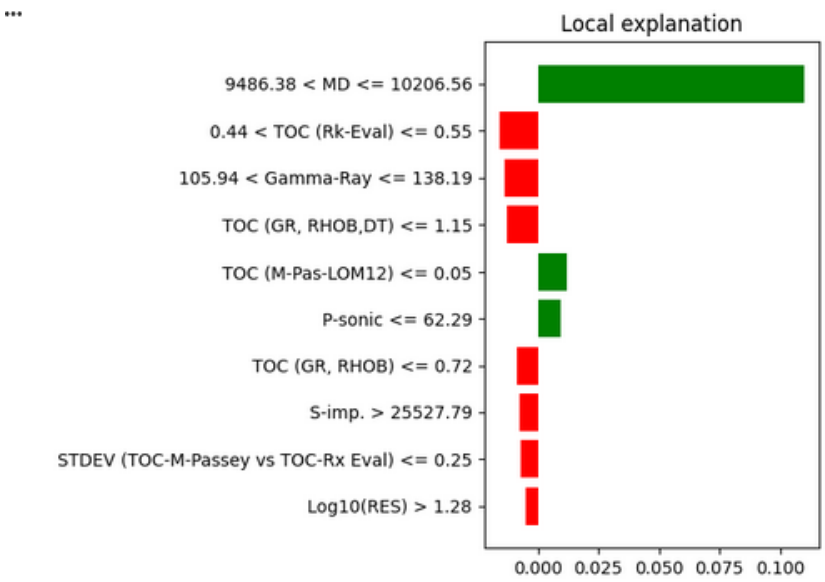
Figures 13: Actual VS Predicted Overlay by Random Forest for TOC-ESTM (KR-3)



Figures 14: SHAP Global Feature Importance for TOC-ESTM (KR-3)



Figures 15: SHAP waterfall plot for TOC-ESTM (KR-3)



Figures 16: LIME explanation for TOC-ESTM (KR-3)

Again, the SHAP global feature importance and the SHAP waterfall plot for TOC-ESTM (KR-3) are shown in Figures 14 and 15.

The SHAP waterfall plot in Figure 15 provides a local explanation of an individual TOC prediction by illustrating how specific features influence the model output relative to the baseline prediction, E[f(X)]=0.573. The final predicted value of f(x)=0.547 is primarily driven by negative contributions from Measured Depth (MD**)** and TOC (Rk-Eval), each reducing the prediction by approximately 0.01 units. Additional minor negative influences are observed from Gamma-Ray, Lambda x Rho, Log10(RES), and R90, while ΔLogR, P-sonic, and RHOB contribute marginal positive effects. The dominance of MD highlights the significance of stratigraphic variation in controlling TOC distribution, whereas the influence of TOC (Rk-Eval) confirms the relevance of geochemically derived indicators in the prediction process. The relatively small contributions from the remaining variables suggest that the model prediction is driven by a limited number of key features rather than a broad set of equally influential predictors.

The local explanation plot for TOC-ESTM (KR-3) in Figure 16 indicate that Measured Depth (MD) is the dominant positive contributor, indicating that the geological interval between 9486.38 and 10206.56 ft is strongly associated with increased TOC values. In contrast, TOC (Rk-Eval), Gamma-Ray, and TOC (GR, RHOB, DT) exert negative influences, reducing the predicted TOC for this observation. Moderate positive contributions are provided by TOC (M-Pas-LOM12) and P-sonic, suggesting that geochemical estimates and acoustic properties contain valuable information for organic richness assessment. Variables such as TOC (GR, RHOB), S-impedance, the standard deviation between Passey and Rk-Eval TOC estimates, and Log10(RES) contribute only marginally to the prediction. The results demonstrate that the model primarily relies on depth-related, geochemical, and petrophysical indicators, while other

attributes provide supplementary information.

The results obtained from the TOC-ESTM (KR-2) and TOC-ESTM (KR-3) datasets demonstrate several similarities and differences in terms of feature relationships, model performance, and explainability outcomes. In both datasets, the correlation analysis revealed the existence of strong interdependencies among petrophysical and TOC-related variables, confirming the presence of complex nonlinear relationships suitable for machine learning-based modelling. The KR-2 dataset exhibited strong correlations among Gamma Ray (GR), Density Transit Time (DT), and Neutron Porosity (NEU), whereas KR-3 displayed stronger associations among elastic and rock-physics attributes such as RHOB, P-sonic, Acoustic Impedance (AI), S-impedance, Poisson's ratio, Lambda x Rho, and Mu x Rho (Nyakill *et al.*, 2022; Khalaf *et al.*, 2026). This suggests that TOC prediction in KR-2 is primarily controlled by conventional petrophysical indicators, while KR-3 incorporates additional elastic properties that capture reservoir heterogeneity.

Regarding predictive performance, Random Forest emerged as the best-performing model for both datasets, confirming the robustness of ensemble learning for TOC estimation. However, the KR-3 dataset achieved substantially higher prediction accuracy ($R^2 = 0.9977$) than KR-2 ($R^2 = 0.9907$), accompanied by significantly lower prediction errors. XGBoost and Decision Tree also performed considerably better on KR-3 than on KR-2, indicating that the KR-3 feature space contains stronger predictive information. Although BiLSTM ranked last in both experiments, its performance improved markedly from KR-2 ($R^2 = 0.5047$) to KR-3 ($R^2 = 0.8552$), suggesting that the richer elastic and geochemical attributes in KR-3 provided additional predictive value even for deep learning models.

The explainability analyses further reveal common trends across KR-2 and KR-3 datasets. SHAP and LIME consistently identified Measured Depth (MD) as the most influential predictor, highlighting the strong stratigraphic control on TOC distribution. Nevertheless, the secondary influential variables differed. In KR-2, ΔLogR, GR, and NEU were identified as major contributors, reflecting the importance of organic richness indicators and conventional well logs. In contrast, KR-3 relied more heavily on TOC (Rk-Eval), P-sonic, Gamma-Ray, and other geochemical and elastic attributes (Nyakill *et al.*, 2022; Khalaf *et al.*, 2026). These differences suggest that TOC prediction mechanisms vary between the two wells due to geological heterogeneity and differences in reservoir characteristics.

Both datasets demonstrate the superiority of ensemble learning methods and the effectiveness of explainable artificial intelligence for transparent TOC prediction. However, the higher predictive accuracy and richer feature interactions observed in KR-3 indicate that integrating petrophysical, elastic, and geochemical attributes provides a more comprehensive representation of reservoir properties than relying primarily on conventional well-log parameters as observed in KR-2. This comparison validates the proposed explainable hybrid framework and highlights the importance of dataset characteristics in determining model performance and interpretability.

Taking into consideration the Nigerian oil and gas sector, accurate Total Organic Carbon (TOC) prediction is critical for evaluating source rock quality, identifying prospective reservoirs, and reducing uncertainties in exploration and production activities. The integration of petrophysical, elastic, and geochemical data enhances reservoir understanding, supports data-driven decision-making, and improves resource evaluation. Furthermore, the use of explainable artificial intelligence (XAI) ensures transparency and trust in predictive models, fostering the adoption of digital technologies that can improve efficiency, and sustainability within Nigeria's petroleum sector.

Conclusion

This study presented an explainable hybrid machine learning and deep learning framework for accurate Total Organic Carbon (TOC) prediction using two datasets, TOC-ESTM (KR-2) and TOC-ESTM (KR-3), derived from the Kolmani River field. The framework integrated feature engineering, multiple predictive algorithms, and explainable artificial intelligence (XAI) techniques to move TOC estimation from a purely black-box modelling paradigm toward a transparent and interpretable decision-support system. Correlation analysis demonstrated the existence of strong nonlinear relationships among petrophysical, elastic, geochemical, and TOC-related variables in both datasets, confirming the suitability of advanced data-driven approaches for reservoir characterization.

The comparative evaluation of Random Forest, Decision Tree, XGBoost, and BiLSTM models revealed that ensemble learning methods consistently outperformed both single-tree and deep learning approaches. Random Forest emerged as the optimal predictor for both datasets, achieving exceptional predictive accuracies of $R^2 = 0.9907$ for KR-2 and $R^2 = 0.9977$ for KR-3, accompanied by the lowest MAE, MSE, RMSE, and MAPE values. These findings demonstrate the ability of Random Forest to effectively capture complex nonlinear interactions among reservoir variables while maintaining excellent generalization performance. Although XGBoost and Decision Tree also produced satisfactory results, they were unable to match the predictive robustness of Random Forest. In contrast, BiLSTM exhibited comparatively weaker performance, particularly in KR-2, highlighting the limitations of deep learning architectures when applied to relatively small and non-sequential well-log datasets.

A major contribution of this study lies in the incorporation of explainable artificial intelligence techniques. The SHAP-based global and local interpretation analyses successfully identified the key drivers of TOC prediction and provided transparent explanations for individual model decisions. Across both datasets, Measured Depth (MD) consistently emerged as the most influential predictor, confirming the strong stratigraphic control on organic matter distribution. However, the secondary controlling variables varied between wells. While KR-2 was predominantly influenced by ΔLogR, Gamma Ray, and Neutron Porosity, KR-3 relied more heavily on geochemical and elastic attributes such as TOC (Rk-Eval), P-sonic, and Gamma Ray. These differences reflect the geological heterogeneity of the studied reservoirs and

demonstrate the capability of explainable models to uncover site-specific controls on TOC distribution. Consequently, the proposed framework not only provides highly accurate predictions but also enhances model trustworthiness, interpretability, and practical applicability for reservoir evaluation and hydrocarbon exploration.

Furthermore, the comparative analysis between KR-2 and KR-3 highlights the importance of feature diversity in TOC modelling. The superior performance achieved in KR-3 suggests that integrating conventional petrophysical logs with elastic and geochemical attributes provides a more comprehensive representation of reservoir characteristics, leading to improved predictive capability. This finding reinforces the value of multidisciplinary data integration in unconventional reservoir studies.

In the future, this proposed framework will be validated using larger and more geographically diverse datasets to assess its robustness and transferability across different sedimentary basins. Again, the integration of seismic attributes, core measurements, and production data may provide additional predictive information and improve reservoir characterization. Again, we plan to explore uncertainty quantification and physics-informed explainable AI approaches to improve prediction reliability and strengthen confidence in operational decision-making.

Acknowledgements

Many thanks to Longman, F. S., Balogun, H., Ojulari, R. O., Olatomiwa, O. J., Balarabe, H. J., Edeh, I. S., & Joshua, O. O. (2024) for an excellent work done and making the data available.

DECLARATIONS

Authors have declared that no competing interests exist.

REFERENCES

Aliouane, L., & Ouadfeul, S. A. (2025). On the capability of multilayer perceptron to predict total organic carbon and elemental capture spectroscopy data in unconventional hydrocarbon reservoirs: The case of the Barnett Shale and Bakken oil field. *Bulletin of Geophysics and Oceanography, 66*(3).

Allouti, S., Michels, R., Mouketo, M. M., Malartre, F., Izart, A., Géraud, Y., De Donato, P., et al. (2025). Total organic carbon evaluation using geophysical well-logs in Lorraine Coal Basin (NE France). *BSGF—Earth Sciences Bulletin, 196*, 24.

Jiang, H., Yang, F., Hu, K., Wang, X., & Liang, Y. (2026). A machine learning-based production prediction method for offshore deep low-permeability to tight reservoirs based on reservoir classification: A case study from the western South China Sea. *Frontiers in Earth Science, 14*, 1804587.

Khalaf, S. M., Fattah, M. M. A., Abdel-Fattah, M. I., Hamdan, H. A., & Abd-Allah, Z. M. (2026). Integrated mineralogical, geochemical, and log-derived TOC evaluation of source rock potential in the Khatatba Formation (Western Desert, Egypt). *Scientific Reports, 16*(1), 19006.

Khan, S., Liu, Z., Lu, Z., Hussain, W., Ahmed, S., Sajid, M., & Imdadullah. (2026). Enhanced estimation of total organic carbon in the Longmaxi Shale Formation using supervised machine learning with lithofacies characterization via K-means clustering. *Carbonates and Evaporites, 41*(2), 59.

Longman, F. S., Balogun, H., Ojulari, R. O., Olatomiwa, O. J., Balarabe, H. J., Edeh, I. S., & Joshua, O. O. (2024). Exploratory analysis of machine learning methods for total organic carbon prediction using well-log data of Kolmani Field. In *Proceedings of the 14th International Conference on Pattern Recognition Systems (ICPRS 2024)* (pp. 1–9). IEEE.

Miao, W., Wang, X., Zhang, W., Qiu, L., Lu, Q., & Gong, X. (2025). Gas sources and productivity-influencing factors of matrix reservoirs in Xujiahe Formation—A case study of Xin 8-5H Well and Xinsheng 204-1H Well. *Processes, 13*(8), 2644.

Nyakilla, E. E., Silingi, S. N., Shen, C., Jun, G., Mulashani, A. K., & Chibura, P. E. (2022). Evaluation of source rock potentiality and prediction of total organic carbon using well log data and integrated methods of multivariate analysis, machine learning, and geochemical analysis. *Natural Resources Research, 31*(1), 619–641.

Passey, Q. R., Bohacs, K. M., Esch, W. L., Klimentidis, R., & Sinha, S. (2010). From oil-prone source rock to gas-producing shale reservoir—Geologic and petrophysical characterization of unconventional shale-gas reservoirs. In *SPE International Oil and Gas Conference and Exhibition in China* (SPE-131350). Society of Petroleum Engineers.

Szabó, N. P., Valadez-Vergara, R., Tapdigli, S., Ugochukwu, A., Szabó, I., & Dobróka, M. (2021). Factor analysis of well logs for total organic carbon estimation in unconventional reservoirs. *Energies, 14*(18), 5978.

Valadez-Vergara, R. (2025). *Well logging method development in unconventional hydrocarbon reservoirs* [Unpublished doctoral dissertation]. Miskolci Egyetem.

Zhang, W., Zhou, S., Chen, R., Liu, D., & Yan, D. (2026). An evaluation of hydrogen adsorption in shale reservoirs using machine learning and SHapley additive exPlanation. *International Journal of Hydrogen Energy, 205*, 153274.

Zhang, X., Yan, L., Lai, F., & Wang, H. (2025). Production prediction for shale oil horizontal wells using convolutional neural network–bidirectional long short-term memory neural network model. *ACS Omega*.